Science of the Total Environment 409 (2011) 1854–1866

Contents lists available at ScienceDirect

Science of the Total Environment

journal homepage: www.elsevier.com/locate/scitotenv

Mechanisms controlling lateral and vertical porewater migration of depleted uranium (DU) at two UK weapons testing sites

Margaret C. Graham [a,*], Ian W. Oliver [b,1], Angus B. MacKenzie [b], Robert M. Ellam [b], John G. Farmer [a]

[a] School of GeoSciences, Crew Building, University of Edinburgh, The King's Buildings, West Mains Road, Edinburgh, EH9 3JN, United Kingdom
[b] Scottish Universities Environmental Research Centre (SUERC), Rankine Avenue, Scottish Enterprise Technology Park, East Kilbride, G75 0QF, United Kingdom

ARTICLE INFO

Article history:
Received 6 October 2010
Received in revised form 23 December 2010
Accepted 6 January 2011
Available online 22 February 2011

Keywords:
Aquatic colloids
Ultrafiltration
Gel electrophoresis
Depleted uranium
Isotopes
Soil contamination

ABSTRACT

Uranium associations with colloidal and truly dissolved soil porewater components from two Ministry of Defence Firing Ranges in the UK were investigated. Porewater samples from 2-cm depth intervals for three soil cores from each of the Dundrennan and Eskmeals ranges were fractionated using centrifugal ultrafiltration (UF) and gel electrophoresis (GE). Soil porewaters from a transect running downslope from the Dundrennan firing area towards a stream (Dunrod Burn) were examined similarly. Uranium concentrations and isotopic composition were determined using Inductively Coupled Plasma-Mass Spectrometry (ICP-MS) and Multi-Collector-Inductively Coupled Plasma-Mass Spectrometry (MC-ICP-MS), respectively.

The soils at Dundrennan were Fe- and Al-rich clay–loam soils whilst at Eskmeals, they were Fe- and Al-poor sandy soils; both, however, had similar organic matter contents due to the presence of a near-surface peaty layer at Eskmeals. These compositional features influenced the porewater composition and indeed the associations of U (and DU). In general, at Dundrennan, U was split between large (100 kDa–0.2 μm) and small (3–30 kDa) organic colloids whilst at Eskmeals, U was mainly in the small colloidal and truly dissolved fractions. Especially below 10 cm depth, association with large Fe/Al/organic colloids was considered to be a precursor to the removal of U from the Dundrennan porewaters to the solid phase. In contrast, the association of U with small organic colloids was largely responsible for inhibiting attenuation in the Eskmeals soils.

Lateral migration of U (and DU) through near-surface Dundrennan soils will involve both large and small colloids but, at depth, transport of the smaller amounts of U remaining in the porewaters may involve large colloids only. For one of the Dundrennan cores the importance of redox-related processes for the re-mobilisation of DU was also indicated as Mn^{IV} reduction resulted in the release of both Mn^{II} and U^{VI} into the truly dissolved phase.

1. Introduction

The long-term behaviour of depleted uranium (DU) in soils in combat and weapons testing zones is an issue of growing concern as the amount of recent literature dedicated to the subject attests (e.g. Di Lella et al., 2004, 2005; Jia et al., 2004, 2005; Johnson et al., 2004; Schimmack et al., 2005, 2007; Alvarez et al., 2006; Oliver et al., 2006, 2007, 2008a,b; Handley-Sidhu et al., 2009a,b,c; Lind et al., 2009; Crancon et al., 2010). Although the risks to the general public are thought to be small (Bem and Bou-Rabee, 2004; Cheng et al., 2004; Oeh et al., 2007; Spratt, 2007; Parrish et al., 2008; Lloyd et al., 2009), there is still considerable uncertainty about the possible long-term health effects associated with DU as a result of internal human exposure (Darolles et al., 2010). Understanding the behaviour and, in particular, the mobility of DU in the vicinity of test-firing sites is therefore of great importance. The potential for leaching and movement of soil and sediment-associated DU has been investigated, to varying degrees, in both field and laboratory studies (Johnson et al., 2004, Jia et al., 2005; Schimmack et al., 2005, 2007; Oliver et al., 2008a; Handley-Sidhu et al., 2009a,b,c), but the processes controlling the retention/release and transport of DU occurring in the natural environment are yet to be fully elucidated.

An investigation conducted by Oliver et al. (2008a) at the Dundrennan Firing Range in SW Scotland found that DU was present in the large (100 kDa–0.2 μm) and small (3–30 kDa) colloid fractions of soil porewater at a distance of some 200 m from the firing area. Moreover, in an analytical precursor study to the current investigation (Graham et al., 2008), organic colloid–DU links in soil porewater were identified as well as a lesser, but potentially important, DU–inorganic colloid association. Such findings are in line with other studies citing the potential importance of porewater colloids for contaminant migration and dispersal (Artinger et al., 2002; Pokrovsky and Schott, 2002; Crancon and Van Der Lee, 2003; Sowder et al., 2003; Lead and Wilkinson, 2006; Mibus et al., 2007; Ranville et al., 2007; Claveranne-Lamolere et al., 2009).

* Corresponding author. Tel.: +44 131 650 4767; fax: +44 131 650 4757.
E-mail address: Margaret.Graham@ed.ac.uk (M.C. Graham).
[1] Current address: Scottish Environment Protection Agency, Riccarton, Edinburgh, EH14 4AP.

0048-9697/$ – see front matter © 2011 Elsevier B.V. All rights reserved.
doi:10.1016/j.scitotenv.2011.01.011

This study explores in finer detail the associations of DU in soil porewater and the mechanisms by which it may migrate both vertically and laterally through soils, including examination of these mechanisms in soils of differing texture (clay–loams to sands). Taking advantage of the differing $^{235}U/^{238}U$ isotopic mass ratios of natural and depleted uranium (atomic mass ratios 0.0072 and ~0.002, respectively), this study employed ultrafiltration (UF), UV–vis, gel electrophoretic (GE) and isotopic analyses to examine the degree of colloidal (organic and inorganic) associations of DU in porewater and its effects on contaminant migration at the study sites.

2. Materials and methods

2.1. Soil sampling locations and collection

Soils were collected during 2006 from the two weapons testing ranges utilised by the UK Ministry of Defence (MoD) for DU munitions research, namely the Dundrennan Firing Range at Kirkcudbright, Scotland, and at the Eskmeals Firing Range, Cumbria, England (Fig. 1a). Details of these locations and their respective weapons testing histories have been published previously (e.g. Oliver et al., 2007) but, in brief, the Raeberry Gun firing position at Dundrennan was a principal DU ammunition test-firing point where DU penetrator shells were tested and refined. Soil contamination, mainly along the firing direction and in the downslope direction from this position (~35 masl) towards a stream known as Dundrod Burn (~5 masl), occurred due to malfunctioning and break-up of the penetrator shells. In contrast, at Eskmeals, DU projectiles were fired at hard target arrays enclosed within a butt (designated VJ Butt). This type of testing exposed the area immediately surrounding the butt to higher levels of DU contamination from aerosols and DU fragments produced on impact. There were also well-characterised differences in soil composition between the Dundrennan and Eskmeals sites. Soil particle size distribution was consistent across all samples from the Dundrennan Firing Range, with values that would identify the soils as clay loams or sandy clay loams (40–55% sand, 20–25% silt, and 22–32% clay). Contrastingly, the soils at the Eskmeals Firing Range were sands (~100% sand) with a thin organic-rich layer at the surface (Oliver et al., 2007). Hydrologically, the soils at Dundrennan were often near-saturated at the surface whilst, at Eskmeals, the soils were well-drained although moist.

At Dundrennan, soil cores were collected from three sites (TP#1–3) along a transect line of increasing distance from the Raeberry Gun firing point (Fig. 1b). TP#1 and TP#2 were collected by excavating soil 'cubes' (~200 $cm^2 \times 21$ cm vertical depth) with a spade and these were sliced on site into 1- or 2-cm depth sections. TP#3 was obtained by digging a pit and pressing a monolith tin, of dimensions 15 cm (open face) × 7 cm breadth × 50 cm length, into the pit wall, after which the core was removed and cut into sections on site. In addition to the soil cores, a bulk surface sample (top 10 cm) was collected at each of TP#1 and TP#2 and also from each of 8 points (BT1-8) along a longer, parallel transect from the Dunrod Burn towards the firing point (Fig. 1b). From Eskmeals, three soil cores were collected using the monolith tin method from locations approximating sites Pad Edge (PE), Waste Storage (WS) and Reference Point (RP), described previously (Oliver et al., 2008b) (Fig. 1c). These three cores were used in an investigation of soil solid phase DU partitioning and further collection details can be found in Oliver et al.

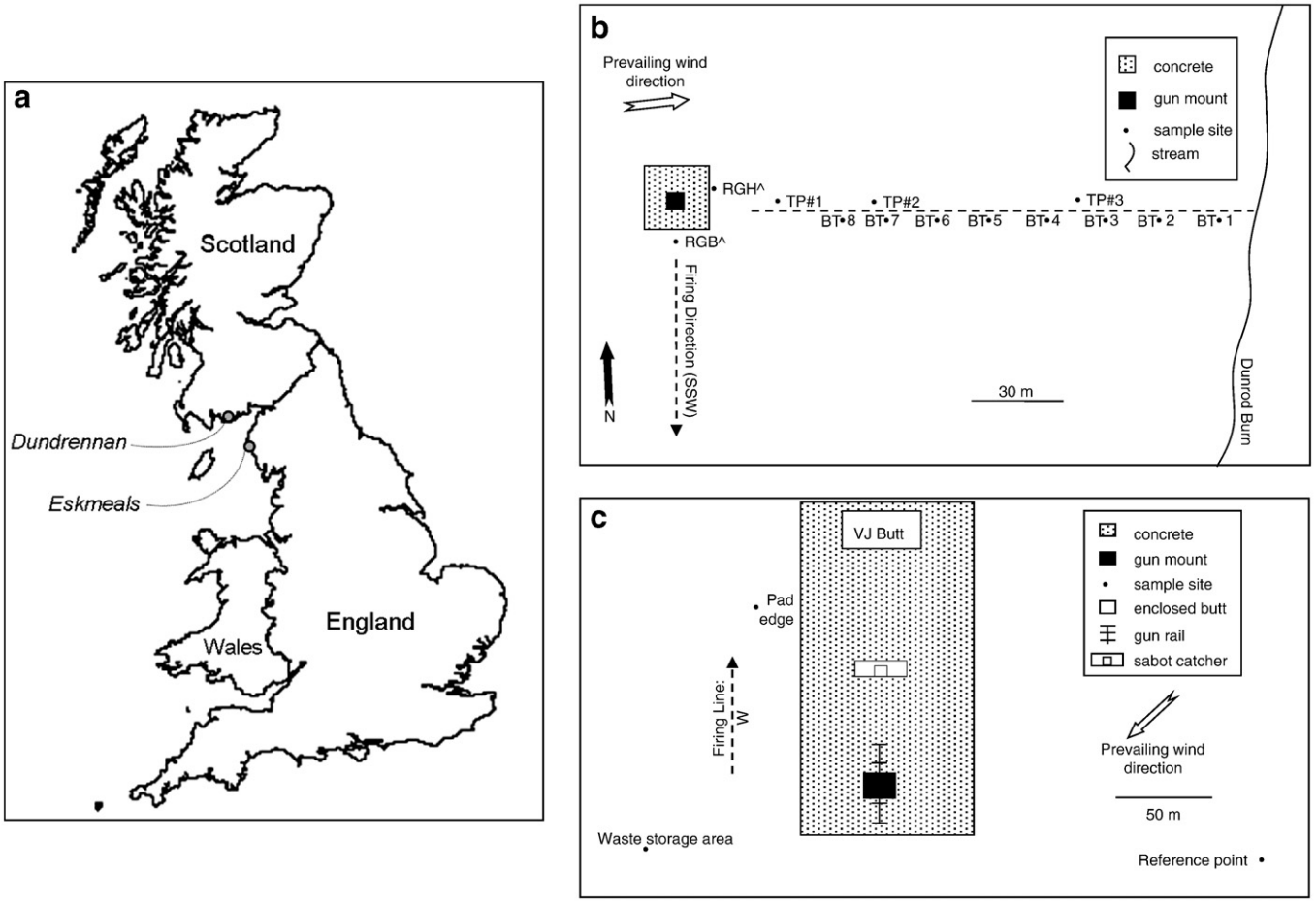

Fig. 1. a. Line map of Great Britain showing the locations of the Dundrennan and Eskmeals Firing Ranges; b: Schematic of the Dundrennan Firing Range, Kirkcudbright, Scotland, showing the 8-point transect line (BT1-8) from Dunrod Burn (BT1: elevation 19 m ASL) to Raeberry Gun (BT8: elevation 33 m ASL) and core (TP#1-3) locations; c: Schematic of VJ Butt, Eskmeals Firing Range, NW England (area shown is within the MoD radiation control zone), showing the core (RP, WS and PE) locations.

(2008b). Once obtained, each individual soil section was placed into a separate polypropylene bag from which air was excluded prior to sealing and transportation to the laboratory, where, after removal of porewaters, the soils were dried, ground and stored as described in Oliver et al. (2008b). Loss on ignition (450 °C; 6 h) was used as a measure of soil organic matter (SOM) content.

2.2. Porewater isolation, filtration, UF and GE examination

The integrated porewater isolation, fractionation and analytical procedure utilised in this investigation has been described previously (Graham et al., 2008). Briefly, soil porewaters were obtained via centrifugation (batches of 50 mL centrifuge tubes, 8873 *g* for 10 min, supernatant filtration through 0.2 μm hydrophilic membranes (Whatman) and bulking of porewaters obtained per sample), with portions of each then allocated to i) acidification and storage at 4 °C for U concentration and isotopic analysis; ii) pH and "dissolved" OM (UV absorbance at 252 nm; Unicam UV2 spectrophotometer) determinations; iii) size separation via centrifugal UF (Vivaspin 20; polyethersulfone membranes; VWR International Ltd, Leicestershire, England) to isolate specific colloid size ranges (100 kDa–0.2 μm, 30–100 kDa, and 3–30 kDa) and <3 kDa 'dissolved' components. Subsamples of each isolated porewater size fraction were also subjected to U concentration and isotopic analysis as described below. The sandy nature of the Eskmeals soils meant that porewaters could not be obtained via direct centrifugation and so a double chamber centrifugation method was employed (adapted from Smolders et al., 1999).

Selected samples from the whole (<0.2 μm) porewaters, UF retentates (i.e. colloids) and <3 kDa solutions obtained were subjected to GE separation as detailed in Graham et al. (2008). In addition to the above samples, whole porewater and porewater size fractions obtained from the parallel eight-point transect line (Fig. 1) established between Raeberry Gun and Dunrod Burn in the sister investigation to this study (Oliver et al., 2008a) were also characterised here using GE.

2.3. Porewater $^{235}U/^{238}U$ isotopic analyses

Whole porewaters and porewater size fractions were analysed for $^{235}U/^{238}U$ isotope mass ratios using a Multi-Collector Inductively Coupled Plasma-Mass Spectrometer (MC-ICP-MS, upgraded Micromass IsoProbe, GV Instruments, UK), according to the method described by Ellam and Keefe (2007).

2.4. Soil U concentration, isotopic signature determination and solid phase partitioning

The U concentrations and $^{235}U/^{238}U$ isotopic signatures of soil solids were determined previously for the three Eskmeals cores (RP, WS and PE) and TP#1 as part of an investigation into the solid phase partitioning of DU in soils (Oliver et al., 2008b). Here, the corresponding values for TP#2 and TP#3 were determined using the same methods.

2.5. Quality control

For accuracy and precision of all U concentration measurements on porewaters (and UF and GE fractions), a 1:10 dilution of the ICP multielement standard solution VI (CertiPUR, Merck) was included in each ICP-OES sample run and measured values were always within ±0.04 of the expected U concentration of 1.00 mg L^{-1}. A 1:100 dilution of this standard was included in each ICP-MS run and the measured values were within ±0.006 of the expected U concentration of 0.100 mg L^{-1}.

To determine the accuracy and precision of concentration measurements for digested soil solids, the International Atomic Energy Agency certified reference soil IAEA-326 was similarly digested, with measured U concentrations (3.2 ± 1 mg kg^{-1}) within standard error of the certified value (2.4 mg kg^{-1}).

Accuracy and precision of the isotopic measurements for soil solids were tested using International Atomic Energy Association certified reference soil IAEA-326, having certified specific activity values for ^{234}U and ^{238}U, with the results being within the stated uncertainties for the certified values.

In addition to determination of isotope activities and activity ratios, the fraction of U in the samples attributable to DU (*f* DU) was computed using a mixing ratio calculation, where the sample U isotope activity ratio ($^{235}U:^{238}U$) was treated as a function of the isotope ratios of natural and depleted U:

$$^{235}U:^{238}U = 0.013 f\mathrm{DU} + 0.046(1 - f\mathrm{DU})$$
$$\therefore f\mathrm{DU} = (0.046 - {}^{235}U:^{238}U)/0.033$$

where $^{235}U:^{238}U$ is the isotope activity ratio of the sample, 0.013 the activity ratio in DU and 0.046 the activity ratio in natural U.

Finally, the methodology for isolation and separation of porewater colloids using ultrafiltration and gel electrophoresis was critically evaluated and validated in Graham et al. (2008).

2.6. Porewater uranium speciation modelling

Porewater uranium speciation modelling was carried out for the PE core depth sections 1.5–3 cm (pH 7.5) and 3–4 cm (pH 6.5) using Visual Minteq 2.50 (with the standard databases that accompany this version of the software).

3. Results

3.1. Porewater composition and elemental concentrations

3.1.1. Soil porewater characterisation

Fig. 2 shows the vertical variations in porewater OM (absorbance at 252 nm), porewater pH and %SOM for the three Dundrennan soil cores (TP#1–3) and the three Eskmeals soil cores (RP, WS and PE).

At Dundrennan, the SOM content decreased from 10–25% (dry wt.) at the surface to 1–4% at the bottom of the cores (Oliver et al., 2008b). In contrast, the porewater OM profiles exhibited more variable depth trends; TP#1 and #2 had subsurface maxima in the 5–10 cm sections, whilst for TP#3 there was a rapid decrease over the top 0–5 cm followed by relatively constant values to ~20 cm but quite variable values thereafter. The porewater pH values were in the range 6.2–8.2 but, although there was an inverse relationship between porewater OM and pH at TP#1, there was no consistent relationship with porewater pH for TP#2–3.

At Eskmeals, the decrease in SOM concentration with increasing depth occurred over the 0–3 cm sections and was generally more rapid than observed at Dundrennan (Oliver et al., 2008b). The high values at the surface (10–23% dry wt.) reflected the peaty surface layer at these locations. Below 10 cm, very much lower concentrations (0.1–2.5% dry wt.) were obtained, as would be expected for sandy soils (Oliver et al., 2008b). The porewater OM profiles for the RP and WS cores both showed surface maxima and then near-constant values below ~5 cm to the bottom of the cores. The profile for the PE core showed only a very slight decrease with depth. The porewater pH values were in the range 5.6–8.1 but only for the WS core was there a clear inverse relationship between porewater OM concentration and pH.

3.1.2. Soil porewater U concentrations

Fig. 2 shows the vertical variations in solid phase soil and soil porewater U concentrations in the Dundrennan (TP#1–3) and Eskmeals (RP, WS, and PE) cores.

At Dundrennan, in TP#1–2 cores, the solid phase U concentrations decreased from ~4–5 mg kg^{-1} in the near-surface sections to ~3–

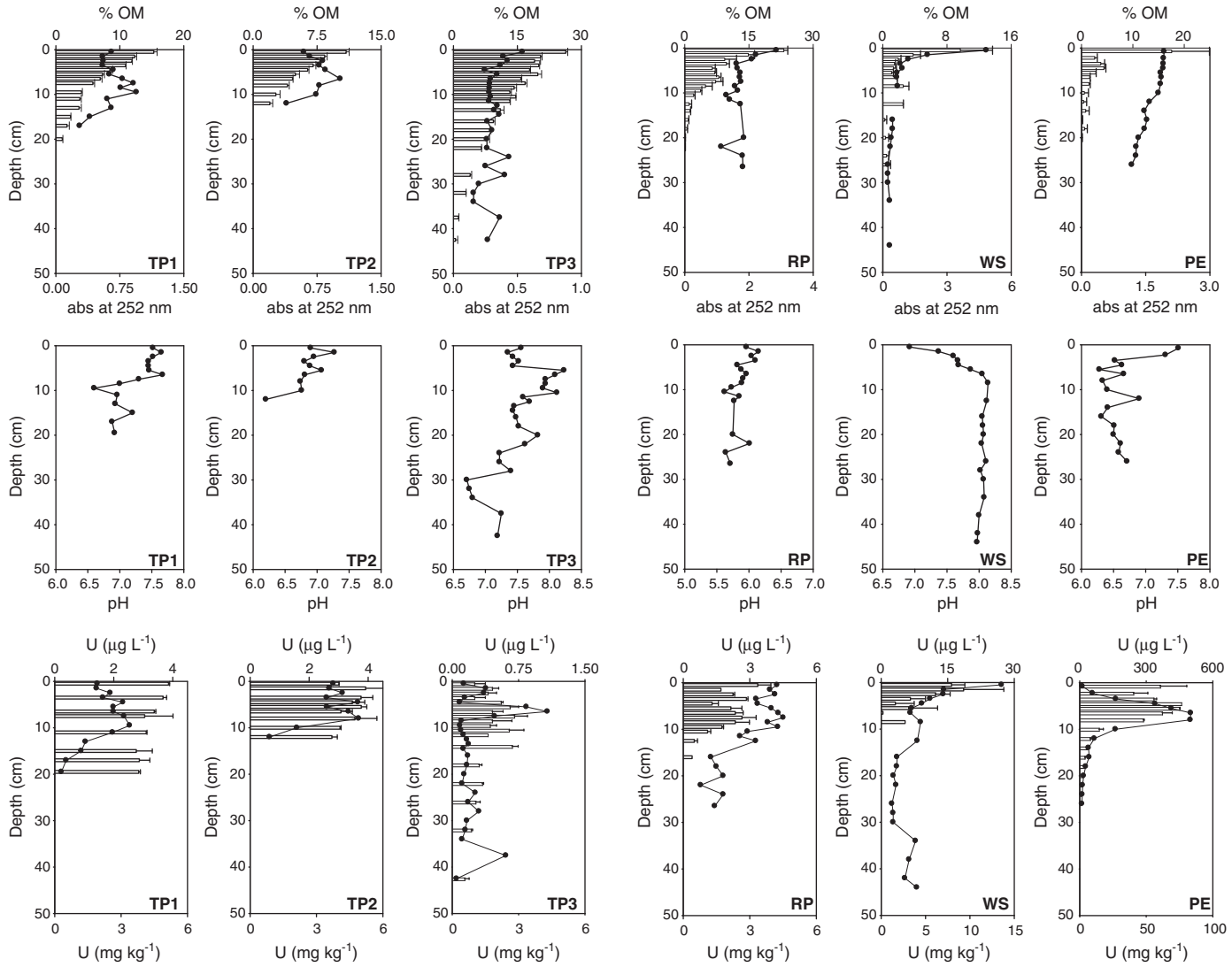

Fig. 2. Porewater OM concentration, pH and U concentration profiles for Dundrennan (TP#1–3) and for Eskmeals (RP, WS, and PE) cores (bars show solid phase OM and U concentrations as published in Oliver et al., 2008b).

4 mg kg^{-1} towards the bottom (Oliver et al., 2008b). In contrast, the U porewater concentrations increased to maxima of ~2.5–3.7 μg L^{-1} at depths of ~8–10 cm and then decreased markedly to ~0.2–0.7 μg L^{-1} towards the bottom of each of these cores. The positions of the porewater U concentration maxima were similar to those for porewater OM concentration. A more complicated pattern was observed for TP#3; there were maxima of ~0.4 μg L^{-1} at 2–3 cm, ~1.1 μg L^{-1} at 6–7 cm and ~0.6 μg L^{-1} at ~35 cm, respectively. The U peak at 6–7 cm coincided with the porewater pH maximum whilst the slight enhancements in the 20–30 cm depth sections and the peak at ~35 cm correlated with increases in porewater OM concentration.

At Eskmeals, the maximum porewater U concentrations (~4.5, 27 and 501 μg L^{-1} for RP, WS and PE, respectively) were typically greater than those at Dundrennan. The maxima always occurred within the top 0–10 cm but the exact depth and extent of the decrease below this point were different for each core. In general, the solid phase concentration profiles also showed higher U concentrations in the 0–10 cm sections and then marked decreases below 10 cm (Oliver et al., 2008b). Calculated mean K_d values (for total U) for each core were in the range 330–500, usually at least an order of magnitude lower than those for the Dundrennan cores (2100–10300). The individual K_d values decreased towards the bottom of each core at RP and WS but remained approximately constant below 10 cm at PE.

3.1.3. Soil porewater DU concentrations

Table 1 contains the soil porewater DU data expressed as the fraction of total uranium represented by DU (*f*DU) and as the actual concentration ([DU]).

At Dundrennan, there was a marked variation in *f*DU between the cores; for TP#1–2, the values were in the range 0.78–0.84 whilst for TP#3, the range was 0.05–0.38. For TP#3, there was also a noticeable trend of decreasing *f*DU from 0.38 at the surface to 0.05 at a depth of 27–29 cm. In the main, [DU] followed these trends; the slightly higher [DU] values at TP#2 compared with those at TP#1 do reflect the higher total U concentrations in the porewater at the former location. However, the calculated K_d values for DU are typically lower than those for total U at comparable depths in TP#2 whilst the K_d values for DU are closer to, but still smaller than, those for total U in the TP#1 core (Table 1). At TP#3, the K_d values for DU are much lower than those calculated for total U (Table 1).

At Eskmeals, *f*DU was in the range 0.91–0.97 for all samples from all of the cores. As a consequence, porewater [DU] and total [U] were almost the same, as were the K_d values for DU and total U.

3.1.4. Soil porewater Mn, Fe, Ca and Mg concentrations

Vertical variations in Mn, Fe, Ca and Mg concentrations for soil porewaters isolated from the Dundrennan (TP#1–3) and Eskmeals

Table 1
Porewater *f*DU, porewater [DU] and K_d values for Dundrennan (TP#1–3) and Eskmeals (RP, WS and PE) cores.

Dundrennan firing range						Eskmeals firing range					
Soil porewater	$^{235}U/^{238}U$	*f*DU[a]	[DU]/μg L^{-1}	K_d (U)[b]	K_d (DU)	Soil porewater	$^{235}U/^{238}U$	*f*DU	[DU]/μg L^{-1}	K_d (U)	K_d (DU)
TP#1						RP					
1–2 cm	0.002836	0.84	1.19	3560 ± 20 (0–1 cm)	2850 ± 16	1–2 cm	0.002319	0.94	3.68	434	388
5–6 cm	0.002955	0.82	1.63	2260 ± 21 (6–7 cm)	1930 ± 15	7–8 cm	0.002335	0.94	4.22	587 ± 47	521 ± 42
TP#2						WS					
1–2 cm	0.002845	0.84	2.26	1950 ± 200	1220 ± 130	1–2 cm	0.002184	0.97	13.7	658 ± 190	625 ± 180
3–4 cm	0.002904	0.83	2.15	1940 ± 120	1310 ± 79						
5–6 cm	0.003170	0.78	2.03	1930 ± 55	1130 ± 32						
TP#3						PE					
1–4 cm	0.005269	0.38	0.10	5150 ± 940 (1–2 cm)	1480 ± 270	1.5–3 cm	0.002446	0.92	53.2	695 ± 110	741 ± 120
5–6 cm	0.005354	0.37	0.31	3100 ± 120	800 ± 71	7–9 cm	0.002198	0.97	484	95 ± 1	95 ± 1
10–11 cm	0.005900	0.27	0.027	25200 ± 3900	5170 ± 790	13–15 cm	0.002360	0.94	37.5	130 ± 8	121 ± 8
27–29 cm	0.007020	0.05	0.015	3350 ± 390 (25–27 cm)	452 ± 53	17–19 cm	0.002470	0.91	24.7	126 ± 27	112 ± 24
TP#1 UF fractions											
100 kDa–0.2 μm		0.84									
3–30 kDa		0.91									
TP#2 UF fractions											
100 kDa–0.2 μm		0.66									
3–30 kDa		0.82									
TP#1 UF fractions											
100 kDa–0.2 μm		0.84									

[a] Typical error on *f*DU < 0.01.
[b] K_d uncertainties calculated using the maximum uncertainty (mean + SE) associated with the solid phase U concentrations.

(RP, WS, and PE) cores are displayed in the supplementary information file (Fig. S1).

3.2. Ultrafiltration (UF) of porewaters and elemental concentrations in colloidal and dissolved porewater fractions

3.2.1. Soil porewater ultrafilter (UF) fractions: uranium

Table 2 shows the percentage of total (<0.2 μm) porewater U in each of the separated colloidal and dissolved components of the porewaters from the Dundrennan (TP#1–3) and Eskmeals (PE) cores. UF recoveries for U were typically >80% and in many cases >90%.

For TP#1 and TP#2, ~60–100% U was present in the large colloid size fraction. At TP#1, the majority of the remainder, ~17–23%, was found in the 3–30 kDa size fraction whilst at TP#2, there was no detectable U in the small colloid/dissolved porewater fractions below 0–1 cm. At TP#3, there was a major change at ~5–6 cm; above and below this depth, a large portion of U (48–73%) was found in the large colloid fraction but at 5–6 cm, almost all of the U was found in the dissolved fraction. This corresponded to the point of maximum porewater U concentration.

For the PE core, the distribution of U was skewed more to the small colloid/dissolved fractions with only 33–46% being present in the large colloid fraction. The proportion of U in the dissolved fraction was particularly high (~33%) in the 0–1 cm porewaters; below this, values were typically in the range 10–20%.

3.2.2. Soil porewater ultrafilter (UF) fractions: DU

For the bulk samples (0–10 cm) collected at TP#1 and TP#2, porewaters were also ultrafiltered and, after appropriate preparation, MC-ICP-MS was used to obtain *f*DU for the separated colloidal and dissolved components. Although all fractions contained significant amounts of DU (in agreement with the overall signature for the porewaters), the 3–30 kDa size fractions contained a slightly higher proportion of DU compared with the 100 kDa–0.2 μm fractions (Table 1). For TP#1, the values for *f*DU were 0.89 for the bulk porewater and 0.84 and 0.91 for the large and small colloids, respectively. For TP#2, the bulk porewater had an *f*DU value of 0.72 and values of 0.66 and 0.82 for the large and small colloids, respectively.

3.2.3. Soil porewater ultrafilter (UF) fractions: OM

Table 2 shows the percentage of total (<0.2 μm) porewater OM in each of the separated colloidal and dissolved components of the porewaters from the Dundrennan (TP#1–3) and Eskmeals (PE) cores. UF recoveries for porewater OM were usually >80% and often >90%.

There was usually a bimodal split of OM between the very large colloid fraction and the small colloid/dissolved fractions (Table 2). The amount of OM in the 30–100 kDa fraction was typically <6% although a few higher values of up to 20% were observed. For TP#1–2, there was a strong correlation between U and OM in the 100 kDa–0.2 μm fraction ($r^2 = 0.76$). The distribution of OM amongst all colloid fractions did not, however, match exactly with that of U. In particular, for the TP#1–3 cores, i.e. the Dundrennan cores, the % OM in the 3–30 kDa fraction was generally greater than the respective % value for U.

At Eskmeals, the bimodal split was skewed more significantly towards the small colloid and dissolved fractions. With increasing soil depth, the amount of OM in the large colloid fraction decreased from 28% to 10–13%.

3.2.4. Soil porewater UF fractions: Al, Fe, Mn, Ca and Mg

Fig. S2 (Supplementary information) shows the distribution of Al, Fe, Mn, Ca and Mg amongst colloidal and dissolved fractions of porewaters from TP#1–3 and PE cores.

3.3. Gel electrophoretic (GE) fractionation and elemental concentrations in GE fractions obtained from porewater colloids

3.3.1. GE fractionation of soil porewater colloids: OM fractionation patterns

Fig. 3 summarises the OM fractionation patterns for total soil porewater colloids (3 kDa–0.2 μm) from TP#1–3. Decreasing size and/or charge results in increased electrophoretic mobility (increased movement from left to right of the gel). There were distinctive between-site differences for the near-surface porewater colloids. TP#1 typically had a prominent relatively mobile brown band (referred to as BB2) and, for certain depth sections, a paler and less mobile brown band (referred to as BB1). TP#2 similarly had BB2 and a more intense and consistent BB1. The TP#3 fractionation patterns did not show either BB1 or BB2, but had a relatively strong band which was only visible under UV light; the fluorescent band (FB) in TP#3 samples and was more mobile than those present in the TP#1–2 samples. Variations with depth were also observed: for TP#1, BB1 increased in intensity whilst for TP#2, BB2 became less prominent in

Table 2
Percentage distribution of U and OM in colloidal and dissolved components of porewaters from Dundrennan (TP#1–3) and Eskmeals (PE) cores.

Depth (cm)	% U (%OM) — TP#1				%U (%OM) — TP#2				% U (%OM) — TP#3				%U (%OM) — PE			
	100 kDa–0.2 μm	30–100 kDa	3–30 kDa	<3 kDa	100 kDa–0.2 μm	30–100 kDa	3–30 kDa	<3 kDa	100 kDa–0.2 μm	30–100 kDa	3–30 kDa	<3 kDa	100 kDa–0.2 μm	30–100 kDa	3–30 kDa	<3 kDa
0–1[a]					62.4 (43.3)	— (—)	16.7 (24.8)	21.4 (31.9)					32.8 (28.1)	2.5 (3.2)	32.4 (28.9)	32.8 (39.8)
2–3[a]	72.9 (50.7)	2.2 (4.9)	16.9 (43.1)	9.0 (1.3)	100 (54.5)	— (1.8)	— (11.0)	— (32.7)	72.5 (50.4)	2.3 (6.9)	10.0 (26.8)	15.2 (15.9)	26.9 (15.9)	4.4 (5.6)	58.8 (43.8)	9.9 (34.8)
4–5					100 (64.0)	— (—)	— (20.1)	— (15.9)					38.9 (18.7)	1.3 (4.2)	44.8 (31.5)	15.0 (45.6)
5–6	73.3 (55.6)	2.0 (—)	20.2 (44.4)	4.5 (—)					0.3 (—)	0.9 (20.9)	3.9 (46.4)	94.9 (32.7)	45.7 (29.2)	1.0 (5.8)	35.0 (28.1)	18.2 (36.7)
6–7	72.1 (39.9)	3.6 (8.6)	18.1 (28.0)	6.2 (23.5)	100 (71.5)	— (—)	— (18.3)	— (10.2)								
7–9	72.8	3.8	20.1	3.3	100	—	—	—								
9–11					100 (66.0)	— (1.8)	— (12.3)	— (19.9)								
11–13													35.4 (9.7)	0.6 (5.6)	41.6 (23.4)	22.4 (61.2)
12–14	80.4		19.6						57.3 (41.7)	1.1 (—)	17.3 (27.2)	24.2 (31.2)				
15–17													43.5 (13.4)	0.6 (2.9)	42.0 (25.6)	13.7 (58.1)
16–18	77.2		22.8													
18–21	86.2	9.3	3.6	—					48.3 (33.6)	3.2 (13.2)	27.4 (42.3)	21.1 (10.9)				
23–25									100	—	—	—				
29–31									100	—	—	—				

[a] 0–1.5 cm and 1.5–3 cm, respectively for pad edge core.

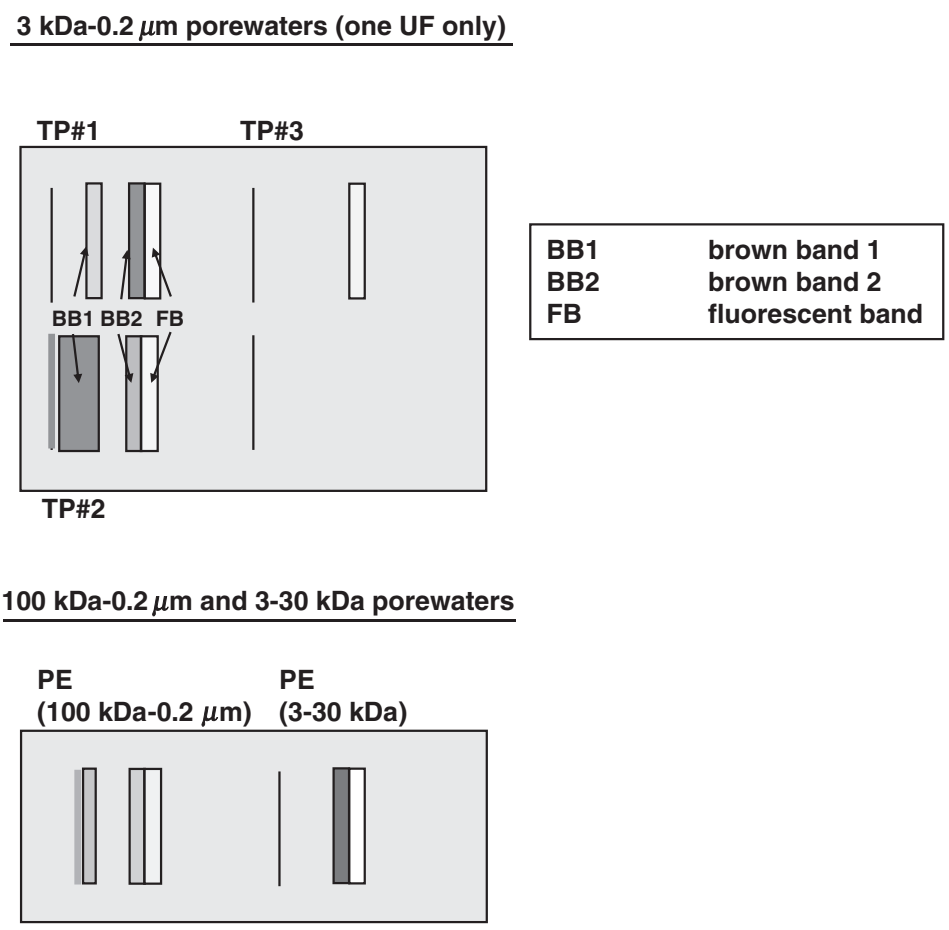

Fig. 3. Schematic showing separation GE patterns achieved for colloids from Dundrennan (TP#1–3) and Eskmeals (PE) porewaters.

comparison with BB1 with increasing soil depth. Brown material was also evident in the gel well TP#2 colloids over the depth range 4–9 cm. At greater depth in TP#3, a pale brown band close to the gel well, in addition to the fluorescent mobile band, was obtained. These depth variations were in good agreement with the OM size distributions obtained by UF.

For the Eskmeals samples, the 100 kDa–0.2 μm and 3–30 kDa colloids (rather than total colloids) from selected depths in the PE core were subjected to GE fractionation. For many of the samples, and for both colloid size ranges, there was only one brown band (BB2) and a fluorescent band, both of which migrated further than the respective bands obtained for the Dundrennan TP#1–2 samples. At each depth, these bands were more intense in the small compared with the large colloid fraction. For the large colloid fraction, there was often brown material which remained in the gel well, e.g. 100 kDa–0.2 μm samples at >10 cm depth.

3.3.2. GE fractionation of soil porewater colloids: U

The GE patterns for total colloids (3 kDa–0.2 μm) for TP#1–3 porewaters from selected soil depths are shown in Fig. 4 (the entire data set is shown in the supplementary information file Fig. S3). In common for all samples was the fact that U did not migrate further than the fluorescent material, the most mobile colloidal component. Moreover, the maximum U concentrations usually coincided with the position of BB1 and/or BB2, giving a strong indication that U in the UF fractions was associated with the OM contained therein. Occasionally, however, the maximum concentration of U occurred in the gel well but this too usually coincided with the observation of brown colouration of the gel well. As for the OM distribution patterns, there were also some variations in U distribution with depth; for TP#1, the increase in intensity of BB1 with increasing depth was reflected by an increase in the amount of coincident U (gel fractions F1/2) and for TP#2, the decrease in intensity of BB2 (and fluorescent band) with increasing depth resulted in marked decrease in the amount of coincident U (gel fractions F4–6). For TP#3, the appearance of a pale brown band (BB1) near the gel well with increasing depth was again accompanied by an increase in the amount of U in gel fraction F1.

For the PE core, the 100 kDa–0.2 μm and the 3–30 kDa UF fractions were separately subjected to GE (Fig. 5). The 100 kDa–0.2 μm patterns showed the presence of U in or close to the gel well, increasingly so for the samples from greater depth, and a large U peak at the position of the pale BB2 and fluorescent band. The 3–30 kDa patterns showed an absence of U in the gel well and a large U peak at the position of the strong BB2 and fluorescent band.

3.3.3. GE fractionation of soil porewater colloids: Fe and Al

The distribution of Fe was sometimes very similar to that of Al, particularly in samples when there was material remaining in the gel well and where the U pattern was skewed back towards the gel well, e.g. TP#2 7–9 cm (Fig. S4). A further interesting feature was that there was almost no Fe/Al at the position of BB2 at any depth.

For the PE core, Fig. S5 shows that the 100 kDa–0.2 μm colloid fractionation pattern for Al and Fe was similar to that observed at Dundrennan, i.e. larger amounts in the gel well where there was brown material remaining there. For the 3–30 kDa fraction, however, there was some additional interesting information; again there was very little Al/Fe present at the position of the brown/fluorescent band but these elements were present in the fractions following on from this, e.g. F7/8, indicating the presence of some small, mobile Al/Fe colloids which do not bind U.

3.3.4. BT transect: GE porewater fractionation: U and OM

The porewaters from selected points on a transect from the Dundrennan firing pad towards Dunrod Burn were also fractionated by UF and GE. The GE patterns for both the 100 kDa–0.2 μm and the 3–30 kDa UF fractions obtained from BT1, 3, 5 and 7 porewaters (0–10 cm) are shown in Fig. 6. Oliver et al. (2008a) demonstrated that the porewater U concentrations generally decreased with distance from the firing pad towards the Dunrod Burn and that DU as a percentage of total U in the porewaters also decreased towards the burn. Moreover, Oliver et al. (2008a) showed that >90% of U was present in colloidal form and

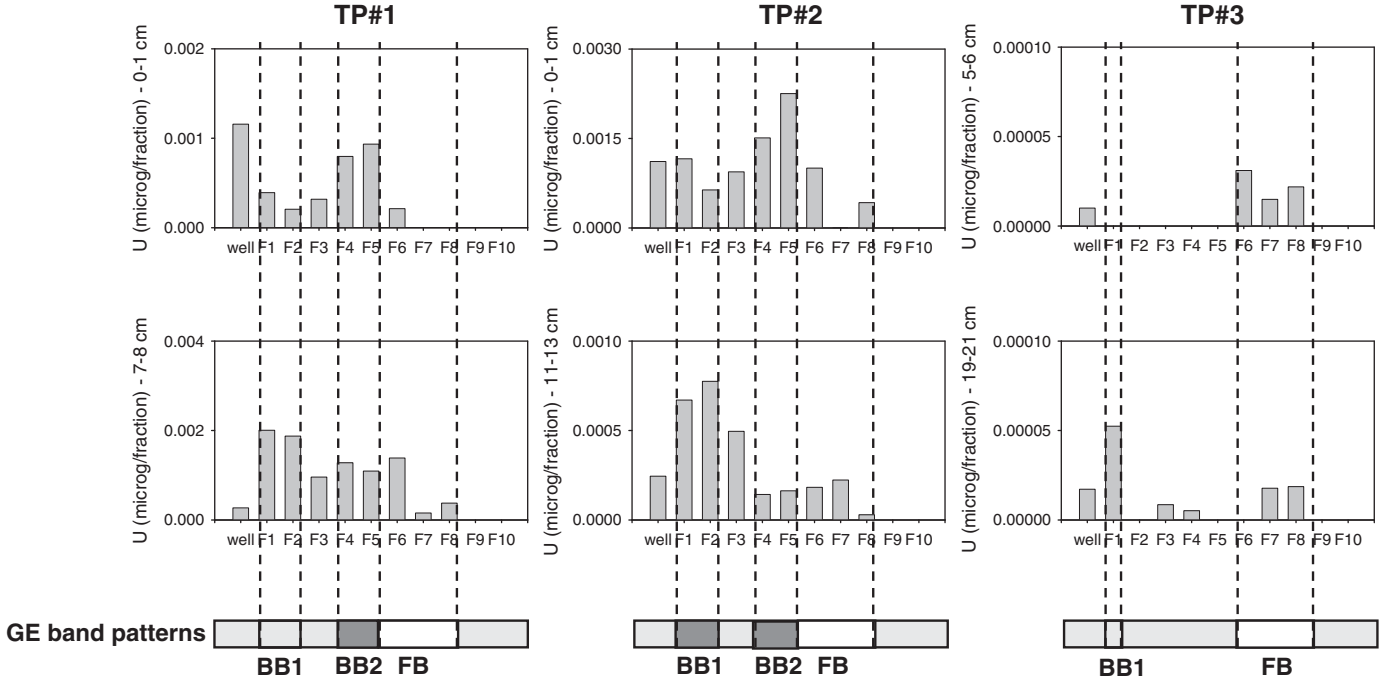

Fig. 4. Gel electrophoretic patterns for U in total porewater colloids (3 kDa–0.2 mm) for Dundrennan (TP#1–3) cores (F1–F10 represent 0.5-cm sections of the gel that have been digested and analysed for elemental concentration).

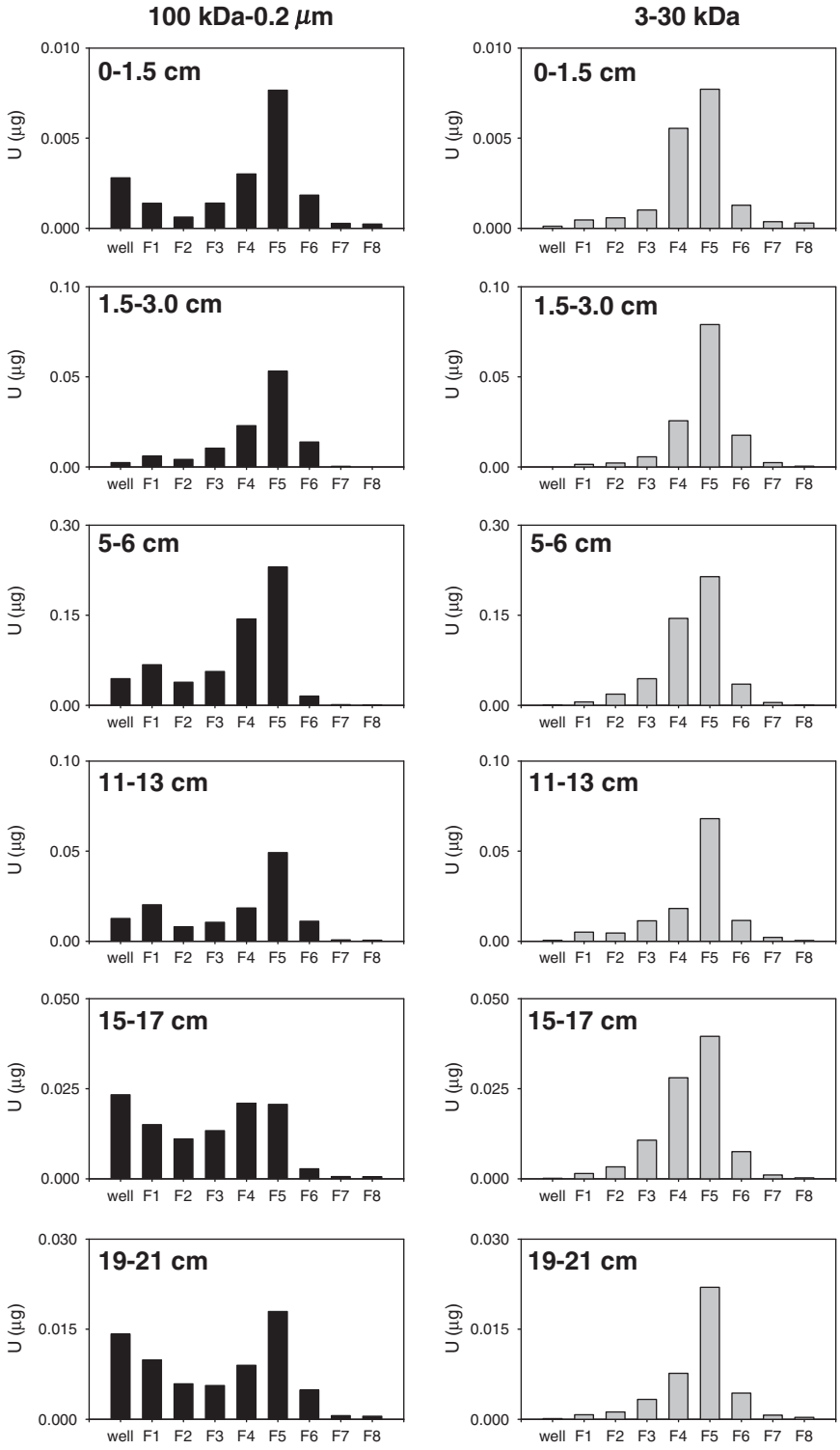

Fig. 5. Gel electrophoretic patterns for U in large (100 kDa–0.2 mm) and small (3–30 kDa) colloids for the PE core.

that this was split between two main fractions (40–80% in the 100 kDa–0.2 μm fraction; 20–50% in the 3–30 kDa fraction). Here, the GE fractionation of the 3–30 kDa and 100 kDa–0.2 μm size fractions showed trends consistent with the UF data published in Oliver et al. (2008a); namely, decreasing U concentration with increasing distance from the firing pad. Within both colloid size fractions, there was also a trend towards U associations with smaller colloids and this also reflected the size distribution of the OM contained therein.

3.4. Quality assurance and analytical considerations

3.4.1. Recoveries from GE: The PE core as an example

Fig. S6 shows the total porewater U concentration and that for the combined GE fractions from the 3–30 kDa and 100 kDa–0.2 μm colloid fractions. The sum of the measured UF porewater U concentrations is also shown. This demonstrates both the good agreement between the UF and GE measurements and also the importance of these two

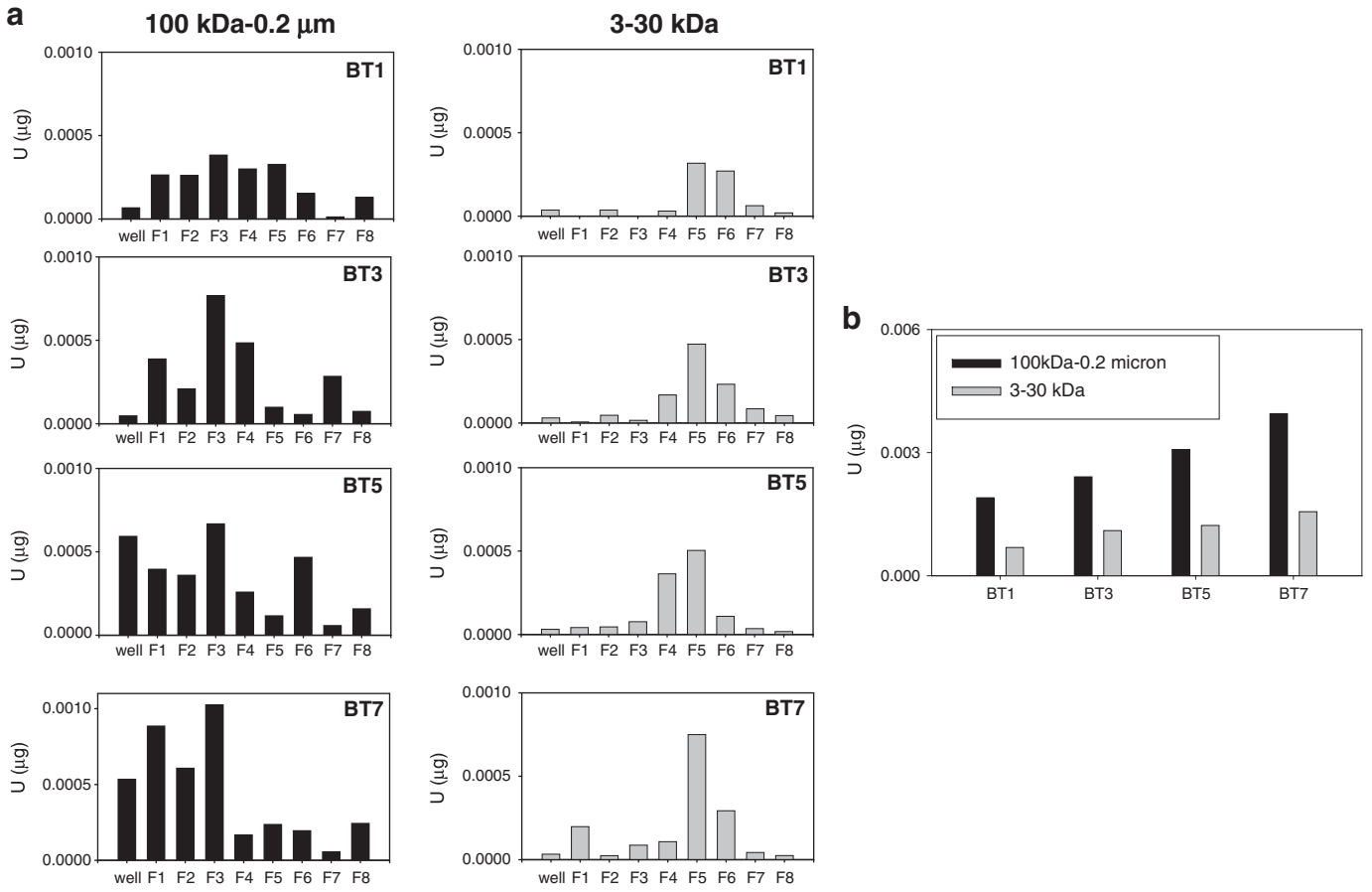

Fig. 6. a) Gel electrophoretic patterns for large (100 kDa–0.2 mm) and small (3–30 kDa) colloids for extended transect points BT 1, 3, 5 and 7 at Dundrennan; b) sum of U in electrophoretic fractions for large and small colloid fractions (Note — BT1 was furthest from, and BT7 was closest to, the firing position).

size fractions in terms of their contribution to total porewater U concentrations.

3.4.2. Other analytical considerations: retention of colloidal and dissolved species by UF

GE fractionation of the total colloid (3 kDa–0.2 µm) fraction obtained by UF led to a very useful observation with respect to U retention: for all samples, U never migrated further than the organic colloidal material present in the sample and a high recovery of U was achieved. This is very significant from an analytical perspective because it shows that the UF method employed in this study did not lead to the retention of large proportions of truly dissolved U as has been encountered for seawater samples (Guo et al., 2007). Dissolved U, present as $UO_2(CO_3)_3^{4-}$ at pH 8.5, would have been highly mobile under the GE conditions employed and so it was concluded that there was little chance that dissolved U had been misidentified as colloidal U in this study.

Comparing GE fractionation patterns for the total colloid fraction with those obtained for 100 kDa–0.2 µm and 3–30 kDa sub-fractions, however, revealed that the 100 kDa UF unit is highly efficient at retaining large colloids but also retains some <100 kDa colloids. This is demonstrated by the presence of BB1 only in the large colloid fraction but the presence of BB2 and the fluorescent band in both large and small colloid fractions for PE porewaters. The strength of BB2 and the fluorescent band present in the 100 kDa–0.2 µm fraction was much less than that in the respective 3–30 kDa fraction, indicating that only a small proportion had been retained by the 100 kDa UF. These findings, however, demonstrate the need for care when using UF as the sole method for colloid fractionation. From this study, we find that UF does reveal the correct general trends, e.g. the colloids at TP#2 are generally larger than those at TP#1 whilst the colloids from the sandy soils at Eskmeals are much smaller in size than those in the porewaters from the loamy soils at Dundrennan. The retention even of a tiny amount of small colloids by the 100 kDa UF, however, can lead to an overestimate of metal associations with the large colloid fraction. If this retention was simply attributable to a less than 100% efficiency in separation, it would be expected that metal retention would be proportional to small colloid retention. The greater metal binding capacity of the small colloids retained by the 100 kDa UF in comparison with those with the same electrophoretic mobility in the 3–30 kDa size fraction may suggest, however, that a selective retention process affecting a small portion of the small colloids may be operating. This will be more fully investigated in future work.

3.4.3. Other analytical considerations: retention of large colloidal material in the gel well during GE

Maximum Fe/Al concentrations often occurred in the gel well, indicating that the Fe/Al colloids were very large/near neutral at pH 8.5. Usually, however, these elevated Fe/Al concentrations coincided with strong brown colouration in the gel well indicating that very large/uncharged humic material was also present. Based on the filtration and gel matrix size cut-off values, the likely size range of the gel well material was ~0.1–0.2 µm. Modifying the conditions employed in gel electrophoresis (increasing the ionic strength of the running buffer to 0.09 M to decrease the hydrodynamic radius of humic colloids; and decreasing the gel pore size by increasing the agarose concentration to 2% w/v so that no large discrete inorganic colloids could enter the gel), however, allowed the gel well material to migrate into the gel. Under these conditions, no material remained in the gel well (Al/Fe/U were not detected) and the brown colour and Al/

Fe/U migrated together, providing evidence for a direct association of OM with the Al/Fe/U (data not shown). Such colloidal associations have previously been suggested by Pokrovsky et al. (2005), who used UF and dialysis rather than the UF/GE methods adopted here.

4. Discussion

4.1. Dundrennan Firing Range: associations of U in soil porewaters

4.1.1. Vertical porewater profiles at TP#1–2

The shapes of the total (<0.2 μm) porewater U and OM concentration profiles were quite similar and there was a moderate correlation between these two parameters ($r^2 = 0.56$; all TP#1–2 data). UF established the distribution of OM, major elements (Al, Fe, and Mn) and U amongst colloidal and dissolved fractions and, in general, it was found that (i) OM was split between the large and small colloids although the exact split depended on both location and soil depth; (ii) Al, Fe and Mn were mainly present in the large colloid fraction; and (iii) U was often split between the large and small colloids (less so for TP#2 than TP#1). Other workers have also identified two populations of colloidal-sized OM and have found U in these organic-rich fractions (e.g. Ranville et al., 2007; Claveranne-Lamolere et al., 2009). For the large colloid fraction in particular, there was a moderately strong correlation between U and OM concentrations ($r^2 = 0.76$; all TP#1–2 data) but the presence of Al, Fe and Mn meant that a direct association of U with OM could not be demonstrated definitively from the UF data per se.

GE fractionation of the entire colloid (3 kDa–0.2 μm) fraction gave OM, Fe/Al and U patterns that were generally consistent with the UF results. For example, the GE patterns often comprised two brown bands, one of low (BB1) and the other of moderate (BB2) electrophoretic mobility. Previous work demonstrated that GE gave a predominantly size-related separation (Graham et al., 2008) and so BB2 comprised smaller colloids than those present in BB1. Importantly, the intensity of BB1 and BB2 matched the large/small colloid split observed following sequential UF of porewaters from selected soil depths. In particular, the decrease in the amount of OM in BB2 and the concomitant increase in the amount of OM in the gel well and in BB1 were consistent with the changes in brown colouration of large and small colloidal size fractions.

The GE patterns for U were usually closely related to those for OM; in particular, the U maxima often coincided with the positions of BB1 and BB2, when present. A main feature was the increasing importance of U association with BB1 and/or gel well material (Fe–Al–humic colloids) with increasing soil depth at both TP#1 and #2. This change is significant with respect to the potential transport of U through soils as lateral water flow through upper sections would lead to loss of U in association with both large and small colloids whilst a similar flow through deeper sections would result in transport of U primarily in association with large colloids. These findings are in broad agreement with Claveranne-Lamolere et al. (2009) who concluded that small humic colloids were important in the near-surface sections whilst larger mineral–organic colloids were important for U transport at depth in soils.

4.1.2. Vertical porewater profiles at TP#3

Quite a different pattern emerged, with subsurface peaks in U, Mn and Ca (and Mg) concentrations at 5–7 cm coinciding with an increase in pH from ~7.5 to ~8.5. UF also revealed a major change in U speciation at this depth, as most of the U was in the dissolved fraction (as was the Ca and Mn) at the point of the U maximum with the remainder being in the 3–30 kDa size fraction. At pH 8.5, $UO_2(CO_3)_3^{4-}$ would be the dominant 'truly dissolved' species in the soil porewaters. As the Mn concentration did not increase towards the soil surface, i.e. indicating plant uptake, the sharp subsurface peak most likely indicates the position of a redox front. In support, there was also an almost exponential decrease in the solid phase Mn concentration below the depth of the porewater maximum (data not shown). Although there has been some consideration of U release during soil Fe redox processes (Thompson et al., 2006), very few studies have considered the effects of reductive dissolution of Mn oxides on U release into the aqueous phase. Importantly, Swarenzski et al. (1999) showed that aqueous U concentrations can be affected by the redox transformation of Mn^{IV} to Mn^{II}; the possible mechanisms in a stratified fjord were complex but the release of U from the surface of Mn^{IV} oxides following reductive dissolution of Mn was thought to be important. Other Mn^{IV}-oxide-associated elements, Sr and Ba, were also released at the same depth as Mn^{II}. Although no Sr or Ba data are available in this study, a sharp increase in both Ca and Mg concentrations was observed at 5–7 cm. A peak in "dissolved" OM at the redox front and a concomitant production of particulate OM-U within the water column led Swarenzski et al. (1999) to conclude that, in addition to redox-related microbial processes, interaction with redox-produced "dissolved" OM may affect U speciation. In our study, however, there was no "dissolved" OM peak in the porewater and the released U was primarily present as truly dissolved species. The predominance of truly dissolved U also suggests that reduction to U^{IV} is unlikely to have occurred. The processes occurring in TP#3 porewaters will be discussed further in Section 4.2.2.

Although there was only a small amount of colloidal U in the TP#3 5–6 cm porewaters, GE fractionation of the total colloid fraction from these porewaters was carried out for comparison with the TP#1–2 samples. This confirmed that the main colloidal association of U at 5–6 cm was with small organic colloids, i.e. consistent with the UF results (Fig. 3 and Table 2), and a similar pattern was obtained for the 6–7 cm porewater colloids (Fig. S3). At greater soil depth, U association with the organic colloids in BB1 was observed and indeed this became the main association at a depth of 19–21 cm. Thus, at depth, it was again shown that large organic colloids would be most important for lateral transport of U.

4.1.3. Variations in U associations in 0–10 cm soil porewaters with increasing distance from the firing pad: BT transect

To establish the wider significance of the U associations at TP#1–2 vs those at TP#3, the porewaters from the 0–10 cm soils at selected points (BT1, 3, 5 and 7) along a transect from the firing pad towards the Dunrod Burn (Fig. 1b) were further characterised using UF and GE. The UF results for the transect porewaters confirmed the presence of both large and small colloids and the association of U with both of these colloidal components (Oliver et al., 2008a). Fe/Al/Mn were found mainly in the large colloid fraction but there were higher concentrations of Fe and Al in BT5–7 than in BT1–3 porewaters, consistent with the observed differences between near-surface TP#1–2 and TP#3 porewaters (Fig. S2). GE fractionation of both the 100 kDa–0.2 μm (large) and the 3–30 kDa (small) colloid fractions revealed further differences between the BT5–7 and BT1–3 porewaters. Within the large colloid fraction, there was a strong association of U with the organic colloids with lowest mobility (gel well and BB1) in the BT5–7 porewaters whilst, for BT1–3, U was associated with a wider range of organic colloids, but was skewed towards those of higher mobility. Within the small colloid fraction, U was often associated with the smaller BB2 organic colloids in both BT5–7 and BT1–3 porewaters. For the latter group, however, there was proportionally more U in the small colloid fraction. Although these patterns represent an average over the top 0–10 cm, they lead to an interpretation of U associations in the porewaters similar to that obtained for the near-surface sections of TP#1–2 and TP#3. Therefore the processes affecting U distribution and associations in the porewaters from these soil cores can be more widely extrapolated to the surface soils extending from the Raeberry Gun firing point downslope towards the Dunrod Burn on the Dundrennan site.

4.2. Dundrennan Firing Range: processes controlling U mobility in soil porewaters

4.2.1. Processes controlling OM, U and DU concentrations in TP#1–2 soil porewaters

The marked decline in solid phase OM and the concomitant increase in predominantly colloidal porewater OM over the top 0–10 cm sections of the soil strongly suggested that release of colloidal OM was occurring as a consequence of the partial decomposition of solid phase OM. Oliver et al. (2008b) showed that ~34% of total U in the soil was bound to solid phase OM in the 0–10 cm sections of the soil. This study has now demonstrated that more than 90% of total porewater U was in the colloidal size range and that there was a direct association of U with both large and small colloidal OM in the porewaters. It is therefore proposed that U is released from the solid phase together with the OM partial decomposition products. DU comprised 76–88% of U bound to solid phase OM and 78–84% of total porewater U in the near-surface sections, and so this would be highly consistent with the proposed release mechanism. Interestingly, the *f*DU results for large and small colloids obtained for porewaters from a 0–10 cm bulk soil collected at both TP#1 and TP#2 suggested that there was a slightly greater proportion of DU in the small colloid (84–91%) than in the large colloid (66–82%) fraction and this could also be significant in enhancing the transport of DU over natural U.

Below 10 cm, there was a decline in porewater OM but the relatively sharper decline in porewater U was suggestive of a decrease in the overall binding capacity of the porewater OM. In support, although only a small amount of data is available for both U and OM in the colloidal fractions, the U/OM concentration ratio for the large colloid fraction decreases from ~7.1–7.2 in the uppermost sections to only ~3.7 in the 9–11 cm section of TP#2. The shift towards larger-sized colloidal OM together with the increasing association of U with large Fe–Al–OM colloids helps to explain why the porewater OM and U concentrations decrease towards the bottom of the cores. It is often considered that formation of larger inorganic–organic colloids is the first step towards removal from the aqueous phase (Filella and Buffle, 1993) and, by a depth of ~12–15 cm, we suggest that the large colloidal associations of U lead to its almost complete removal from the porewaters.

4.2.2. Processes controlling OM, U and DU concentrations in TP#3 soil porewaters

Although the solid phase OM concentrations are higher than those in the surface sections of TP#1–2, the porewaters at TP#3 were considerably paler in colour and contained significantly lower proportions of large organic colloids. Indeed, the porewaters from the 5–7 cm sections, the position of the Mn^{IV}/Mn^{II} boundary, were almost colourless. We propose that the release of U associated with (i) Mn^{IV} oxides upon reductive dissolution and/or (ii) solid phase OM that has undergone complete mineralization are the two most likely processes occurring in these sections of TP#3. In support of this postulate are the previously unpublished sequential extraction data for the solid phase of this core which showed that about 60–70% of U and Mn was extracted in the reducible step with most of the remainder of each having been extracted in the exchangeable step (Fig. S7). Significantly, this demonstrated a close relationship between U and Mn.

Our GE results again suggest that OM alteration processes result in increasingly large colloidal OM with increasing soil depth, which would be expected ultimately to result in the removal of OM and associated U from the porewater. At depth, however, there is very little DU in the solid phase and only 5% of the total porewater U at 27–29 cm is DU. At this location, it is therefore the redox-related processes occurring in the top 0–10 cm of the soil, where DU comprises 30–40% and 27–38% of total U in the soil and porewaters, respectively, that are most important in controlling its fate. In particular, DU that has been attenuated in the upper sections of solid phase soil, either by direct interaction with Mn oxides or with solid phase OM, will be re-released into soil porewaters as conditions become mildly reducing (sufficient for Mn reduction). The K_d values for DU are much lower than those for U, indicating that the soils at TP#3 have a much lower ability to retain DU than those at TP#1–2 and this is probably attributable to the prevailing redox conditions in combination with the composition of OM.

4.3. Eskmeals Firing Range: associations of U in soil porewaters

4.3.1. Vertical porewater profiles at PE

To investigate the vertical mobility of DU in a different solid matrix, the PE core was selected for porewater characterisation by UF and GE. A thin peaty layer overlays the predominantly sandy soil and, as a consequence, porewater OM was readily measurable at all depths. The UF data again revealed a bimodal split but much more OM was in the small colloid and dissolved fractions compared with the Dundrennan TP#1–3 samples. Since the solid phase Fe and Al contents of the sandy soils were generally much lower (unpublished data), larger Fe/Al/organic colloids would be expected to be less prominent. The UF data also showed that there was much more U present in the smaller colloid and dissolved fractions compared with the Dundrennan soils. There was no distinct trend in the colloidal associations of U with increasing depth but there was a general decrease in the amount of truly dissolved U (<3 kDa). The GE fractionation of the large (100 kDa–0.2 μm) and small (3–30 kDa) colloid fractions did, however, provide additional information about the nature of the colloids within these two size ranges. For both, BB2 was the main feature of the gel viewed under visible light and, following from the analytical considerations presented in Section 3.4.3, it will be assumed that the component present in the large colloid fraction has been retained due to an inefficient removal of the small organic colloids comprising BB2. Importantly, the main association of U was with these small organic colloids which have very little associated Fe or Al. BB1 was only present in the large colloid fraction gel patterns and was generally pale brown in colour. Although still representing a minor association, for the large colloid fraction there was also a small but increasing amount of U in the gel well (Fe–Al–humic colloids) and at the position of BB1 with increasing soil depth, i.e. similar to the depth trend observed for the three Dundrennan soil cores, TP#1–3.

4.4. Eskmeals Firing Range: processes controlling U mobility in soil porewaters

4.4.1. Processes controlling OM, U and DU concentrations in PE soil porewaters

The major forms of U in the porewaters were (i) truly dissolved, e.g. $Ca_2UO_2(CO_3)_3^0$, $(UO_2)_2(CO_3)(OH)_3^-$, $UO_2(CO_3)^0$, $UO_2(CO_3)_2^{2-}$ at pH 7.5; (ii) small organic colloidal U (3–30 kDa); (iii) large Fe/Al/organic- and large organic–colloidal U (100 kDa–0.2 μm). The elevated pH (7.5) accounts for the higher proportion of truly dissolved U in the top section in comparison with the immediately underlying section where pH dips to 6.5. Below this, the pH increased towards 7 and the proportion of truly dissolved U again increased, providing further evidence for the pH control on U speciation at this location. The porewater OM concentrations decreased only slowly with increasing depth and it was therefore not surprising that the dominant form of U at all depths was an organic colloidal form, most commonly a direct interaction with small humic colloids. Over the top 0–20 cm, DU comprised >90% of the total porewater U and so this work provides strong evidence for the vertical transport of DU at this site in association with small organic colloids with which there was little associated Fe/Al. There were some small Fe/Al colloids, predominantly in the 3–30 kDa size fraction, but these were

more electrophoretically mobile than the BB2 OM and had no associated U.

During vertical transport, both immobilisation and mobilisation of DU may occur via several mechanisms which are dependent on the conditions prevailing in the porewaters. For example, at pH>5, soluble U^{VI} species have been shown to be immobilised in subsurface materials by sorption or co-precipitation reactions (e.g. Abedoulas et al., 1998; Camus et al., 1999). For lower pH values, humic aggregates are considered to be responsible for the strong immobilisation of uranium in soil (Crancon and Van Der Lee, 2003). For the PE porewaters in this study, pH values in the range 6.5–7.5 suggest that aggregation of humic colloids would be unlikely to occur and so immobilisation, should it occur, would most likely be effected via sorption or co-precipitation reactions.

Alternatively, mobilisation of DU following water infiltration has been attributed to a partial reversal of sorption reactions in response to a decrease in porewater ionic strength (e.g. Gabriel et al., 1998; Zheng and Wan 2005). Rainwater infiltration can also affect other solution properties, e.g. a lowering of pH is not uncommon. For the PE porewaters, however, the highest concentrations of major ions such as Ca^{2+} and indeed the highest pH values (~7.5) were obtained for the 0–1.5 cm section. It is therefore unlikely that rainwater infiltration has altered U speciation in the PE core. It is hypothesized that the thin peaty layer on the surface of the Eskmeals cores may act as a "buffer" with respect to rainwater infiltration-induced changes in porewater properties.

From the sequential extraction results for the solid phase (Oliver et al., 2008b), there was a major change in the solid phase U associations with increasing depth in the PE core. In the top 0–10 cm sections, more than 70% U was present in the residual fraction with most of the remainder being associated with SOM. In the 10–20 cm section, U was split amongst the exchangeable (~22%), Fe/Mn oxide (~41%) and SOM (~38%) fractions, and below 20 cm there was a further shift to 100% association with SOM. It is proposed that weathering processes are gradually releasing DU from the contamination source in the 0–10 cm sections (probably uranium oxides and weathering products, schoepite and metaschoepite etc., e.g. Handley-Sidhu et al., 2009c; Crancon et al., 2010) into the porewaters. The downwards displacement of the porewater U maximum from that present in the solid phase is suggestive of the effect of waters percolating down through the sand. Some of the released DU may be immediately complexed by solid phase OM as indicated by the sequential extraction results but this study has shown that, in the porewaters, a significant amount becomes complexed by the small humic colloids and some remains in the 'truly dissolved' fraction. By passing U and humic acids through a sand-filled column, Mibus et al. (2007) concluded that a kinetic filtration process continuously removes humic colloids from the advective flow. They assumed that U^{VI} was withdrawn along with the humic colloids onto the surfaces of the quartz sand particles. The results of our study would be consistent with several removal mechanisms: (i) weak interaction of "dissolved U" with quartz surfaces, leading to "exchangeable U" in the solid phase; (ii) stronger sorption of U–organic colloids onto the solid phase, leading to "oxidisable U" in the solid phase; (iii) sorption of "dissolved U" to Fe/Mn secondary minerals, leading to "reducible U" in the solid phase. At 10–20 cm depth, removal of dissolved U by all three mechanisms would be consistent with both the sequential extraction and porewater speciation results. From 10 cm depth but particularly below 20 cm depth, the major removal process involves sorption/precipitation of U–OM colloids onto the solid phase. The GE results for the porewaters provide evidence for the presence of very large Fe/Al–U–OM colloids with increasing depth; as discussed in preceding sections, these may be precursors of the forms of U that are being removed to the solid phase. Overall, the removal processes do not fully attenuate DU and the evidence that we have gathered strongly suggests that it is the binding of U to small organic colloids that is the main process inhibiting attenuation. The high stability of U^{VI}–humate complexes has previously been reported (e.g. Artinger et al., 2002) and we conclude that it is specifically small DU–humic complexes that are implicated in the enhanced migration of DU through these sandy matrices.

Finally, the long-term fate of DU may depend on the nature of its interactions with the solid phase, i.e. held at exchangeable sites, bound to organic matter which has sorbed to minerals, bound to Fe/Mn oxides. Exchangeable forms may be re-released following changes in ionic strength and other solution properties of the porewater, the mobility of sorbed DU–humic complexes may be sensitive to changes in soil moisture and the velocity and chemistry of the water phase (e.g. Kretschmar and Sticher, 1997; Crancon et al., 2010) whilst DU held at Fe/Mn oxide surfaces may be susceptible to re-release upon reductive dissolution of the oxides.

5. Conclusions

Although this study has revealed some site-specific behaviour of DU, a number of unifying features were observed. For both the clay–loam and sandy soils at Dundrennan and Eskmeals, respectively, the behaviour of U and DU was strongly influenced by processes affecting the distribution of humic substances between the solid phase and soil porewaters. In some cases, redox processes were also intimately involved. Specifically:

(1) In the near-surface sections of the TP#1–2 soils, U was associated with both large (100 kDa–0.2 μm) and small (3–30 kDa) organic colloids, whereas towards the bottom of the cores U was predominantly associated with the large colloids, including Fe/Al/humic colloids.
(2) Organic colloids are released into the porewaters as a consequence of partial decomposition of solid phase organic matter. Although two discrete size ranges were found in near-surface samples, larger colloids were increasingly prevalent at depth and very large Fe/Al/humic colloids were sometimes observed. Formation of such colloids is a likely first step towards their removal from the aqueous phase and it was concluded that U association with such colloids promoted its transfer to the solid phase soil.
(3) In the near-surface sections of TP#3 the porewaters were less strongly coloured and there was also a major change in U speciation at 5–7 cm depth, the position of the Mn^{IV}/Mn^{II} redox front. It was proposed that reductive dissolution of Mn oxides and decomposition of OM led to the release of dissolved uranyl carbonate species. Towards the bottom of the core, U was again predominantly associated with large organic colloids.
(4) Importantly, large and small organic colloids were implicated in the transport of DU through the near-surface soils. A proportion of this DU is retained by soils along this transect but, even at a distance of ~200 m from the firing area, DU comprised ~27% of porewater U in near-surface soils.
(5) In sandy soils at Eskmeals, which were overlain by a thin peaty layer, there was significantly more low molecular weight colloidal and dissolved OM; accordingly, DU in the PE porewaters was more prevalent in the small colloidal and dissolved fractions.
(6) For the PE core, a slightly greater association of U with low mobility colloids within the large colloid fraction occurred with increasing depth but the major interaction at all depths was with small organic colloids which had very little associated Fe/Al.
(7) Since the proportion of U in dissolved form decreased with increasing depth, association with small organic colloids became increasingly important for maintaining U concentrations in excess of 10 $\mu g\,L^{-1}$ at depths down to 26 cm in the PE porewaters.

Acknowledgements

This study was enabled though the support of the Natural Environment Research Council (NERC, grant NE/C513134/1) and the co-operation of the UK MoD and QinetiQ. We also thank K. Keefe for technical assistance with multi-collector ICP-MS analyses.

Appendix A. Supplementary data

Supplementary data to this article can be found online at doi:10.1016/j.scitotenv.2011.01.011.

References

Abedoulas A, Lutze W, Nuttall E. Chemical reactions of uranium in ground water at a mill tailings site. J Contam Hydrol 1998;34:343–61.
Alvarez R, Livens FR, Lloyd JR, Vaughan DJ. Biogeochemical influences on the decomposition and dispersion of depleted uranium in the environment. Geochim Cosmochim Acta 2006;70:A12.
Artinger R, Rabung T, Kim JI, Sachs S, Schmeide K, et al. Humic-colloid borne migration of uranium in sand columns. J Contam Hydrol 2002;58:1-12.
Bem H, Bou-Rabee F. Environmental and health consequences of depleted uranium use in the 1991 Gulf War. Environ Internat 2004;30:123–34.
Camus H, Little R, Acton D, Agüero A, Chambers D, Chamney L, et al. Long-term contaminant migration and impacts from uranium mill tailings. J Environ Radioact 1999;42:289–304.
Cheng J-J, Hlohowskyj I, Chih LT. Ecological risk assessment of radiological exposure to depleted uranium in soils at a weapons testing facility. Soil Sed Contam 2004;13: 579–95.
Claveranne-Lamolere C, Lespes G, Dubascoux S, Aupais J, Pointurier F, et al. Colloidal transport of uranium in soil: size fractionation and characterisation by field-flow fractionation-multi-detection. J Chrom A 2009;1216:9113–9.
Crancon P, Van Der Lee J. Speciation and mobility of uranium (VI) in humic-containing soils. Radiochim Acta 2003;91:673–9.
Crancon P, Pili E, Charlet L. Uranium facilitated transport by water-dispersible colloids in field and soil columns. Sci Total Environ 2010;408:2118–28.
Darolles C, Broggio D, Feugier A, Frelon S, Dublineau I, et al. Different genotoxic profiles between depleted and enriched uranium. Toxicol Lett 2010;192:337–48.
Di Lella LA, Tratti L, Loppi S, Protano G, Riccobono F. Environmental distribution of uranium and other trace elements at selected Kosovo sites. Chemos 2004;56:861–5.
Di Lella LA, Nannoni F, Protano G, Riccobono F. Uranium contents and $^{235}U/^{238}U$ atom ratios in soil and earthworms. Sci Total Environ 2005;227:109–18.
Ellam RM, Keefe KJ. Uranium isotope ratios using a $^{229}Th/^{232}Th$ external mass bias correction. J Anal At Spectrom 2007;22:147–52.
Filella M, Buffle J. Factors controlling the stability of submicron colloids in natural waters. Colloids Surf A Physicochem Eng Aspects 1993;73:255–73.
Gabriel U, Gaudet JP, Spadini L, Charlet L. Reactive transport of uranyl in a goethite column: an experimental and modelling study. Chem Geol 1998;151:107–28.
Graham MC, Oliver IW, MacKenzie AB, Ellam RM, Farmer JG. Combined use of GE, UF and gel filtration fractionation of colloidal humic substances for the investigation of uranium–humic substance interactions at a depleted uranium weapons testing site. Sci Total Environ 2008;404:207–17.
Guo L, Warnken KW, Santschi PH. Retention behaviour of dissolved uranium during ultrafiltration: implications for colloidal uranium in surface waters. Mar Chem 2007;107:156–66.
Handley-Sidhu S, Worsfold PJ, Boothman C, Lloyd JR, Alvarez R, et al. Corrosion and fate of depleted uranium penetrators under progressively anaerobic conditions in estuarine sediments. Environ Sci Technol 2009a;43:350–5.
Handley-Sidhu S, Worsfold PJ, Livens FR, Vaughan DJ, Lloyd JR, et al. Biogeochemical controls on the corrosion of depleted uranium alloy in subsurface soils. Environ Sci Technol 2009b;43:6177–82.
Handley-Sidhu S, Bryan ND, Worsfold PJ, Vaughan DJ, Livens FR, et al. Corrosion and transport of depleted uranium in sand-rich environments. Chemos 2009c;77:1434–9.
Jia G, Belli M, Sansone U, Rosamilia S, Gaudino SJ. Concentration, distribution and characterization of depleted uranium (DU) in the Kosovo ecosystem: a comparison with the uranium behaviour in the environment uncontaminated by DU. Radioanal Nucl Chem 2004;260:481–94.
Jia G, Belli M, Sansone U, Rosamilia S, Gaudino S. Concentration and characteristics of depleted uranium in water, air and biological samples collected in Serbia and Montenegro. Appl Rad Isot 2005;63:381–99.
Johnson WH, Buck BJ, Brogonia H, Brock AL. Variations in depleted uranium sorption and solubility with depth in arid soils. Soil Sed Contam 2004;13:533–44.
Kretschmar R, Sticher H. Transport of humic-coated iron oxide colloids in a sandy soil: influence of Ca^{2+} and trace metals. Environ Sci Technol 1997;31:3497–504.
Lead JR, Wilkinson KJ. Aquatic colloids and nanoparticles: current knowledge and future trends. Environ Chem 2006;3:159–71.
Lind OC, Salbu B, Skipperud L, Janssens K, Janoszewicz J, et al. Solid state speciation and potential bioavailability of depleted uranium particles from Kosovo and Kuwait. J Environ Rad 2009;100:301–7.
Lloyd NS, Chenery T, Parrish RR. The distribution of depleted uranium contamination in Colonie, NY, USA. Sci Total Environ 2009;408:397–407.
Mibus J, Sachs S, Pfingsten W, Nebelung C, Bernhard G. Migration of uranium(IV)/(VI) in the presence of humic acids in quartz sand: a laboratory column study. J Contam Hydrol 2007;89:199–217.
Oeh U, Priest ND, Roth P, Ragnarsdottir KV, Li WB, et al. Measurement of daily urinary excretion in German peacekeeping personnel and residents of the Kosovo region to assess potential intake of depleted uranium. Sci Total Environ 2007;381:77–87.
Oliver IW, MacKenzie AB, Ellam RM, Graham MC, Farmer JG. Determining the extent of depleted uranium contamination in soils at a weapons test site: an isotopic investigation. Geochim Cosmochim Acta 2006;70:A457.
Oliver IW, Graham MC, MacKenzie AB, Ellam RM, Farmer JG. Assessing depleted uranium (DU) contamination of soil, plants and earthworms at UK weapons testing sites. J Environ Monit 2007;9:740–8.
Oliver IW, Graham MC, MacKenzie AB, Ellam RM, Farmer JG. Depleted uranium (DU) mobility across a weapons testing site: isotopic investigation of porewater, earthworms and soils. Environ Sci Technol 2008a;42:9158–64.
Oliver IW, Graham MC, MacKenzie AB, Ellam RM, Farmer JG. Distribution and partitioning of depleted uranium in soils at weapon test ranges — investigations combining the BCR extraction scheme and isotopic analysis. Chemos 2008b;72: 932–9.
Parrish RR, Harstwood M, Arnason JG, Chenery S, Brewer T, et al. Depleted uranium contamination by inhalation exposure and its detection after 20 years: implications for human health assessment. Sci Total Environ 2008;390:58–68.
Pokrovsky OS, Schott J. Iron colloids/organic matter associated transport of major and trace elements in small boreal rivers and their estuaries (NW Russia). Chem Geol 2002;190:141–79.
Pokrovsky OS, Dupre B, Schott J. Fe–Al–organic colloids control of trace elements in peat soil solutions: results of UF and dialysis. Aquat Geochem 2005;11:241–78.
Ranville JF, Hendry MJ, Reszat TN, Xie Q, Honeyman BD. Quantifying uranium complexation by groundwater dissolved organic carbon using asymmetrical flow field-flow fractionation. J Contam Hydrol 2007;91:233–46.
Schimmack W, Gerstmann U, Oeh U, Schultz W, Schramel P. Leaching of depleted uranium in soils as determined by column experiments. Rad Environ Biophys 2005;44:183–91.
Schimmack W, Gerstmann U, Schultz W, Geipel G. Long-term corrosion and leaching of depleted uranium (DU) in soil. Rad Environ Biophys 2007;46:221–7.
Smolders E, Brans K, Foldi A, Merckx R. Cadmium fixation in soils measured by isotope dilution. Soil Sci Soc Am J 1999;63:78–85.
Sowder AG, Bertsch PM, Morris PJ. Partitioning and availability of uranium and nickel in contaminated riparian sediments. J Environ Qual 2003;32:885–98.
Spratt BG. Health hazards of depleted uranium munitions: estimates of exposures and risks in the Gulf war, the Balkans, and Iraq. In: Miller AC, editor. Depleted uranium: Properties, uses, and health consequences. Boca Raton: Taylor and Francis; 2007. p. 121–41.
Swarenzski PW, McKee BA, Skei JM, Todd JF. Uranium biogeochemistry across the redox transition zone of a permanently stratified fjord: Framvaren, Norway. Mar Chem 1999;67:181–98.
Thompson A, Chadwick OA, Boman S, Chorover J. Colloid mobilization during soil iron redox oscillations. Environ Sci Technol 2006;40:5743–9.
Zheng ZP, Wan JM. Release of contaminant U(VI) from soils. Radiochim Acta 2005;93: 211–7.